

An optimized algebraic basis for molecular potentials.

Andrea Bordoni* and Nicola Manini

Dipartimento di Fisica, Università di Milano,

Via Celoria 16, 20133 Milano, Italy

July 27 2007

Abstract

The computation of vibrational spectra of diatomic molecules through the exact diagonalization of algebraically determined matrixes based on powers of Morse coordinates is made substantially more efficient by choosing a properly adapted quantum-mechanical basis, specifically tuned to the molecular potential. A substantial improvement is achieved while still retaining the full advantage of the simplicity and numerical light-weightedness of an algebraic approach. In the scheme

*Corresponding author. E-mail: andrea.bordoni@unimi.it

we propose, the basis is parameterized by two quantities which can be adjusted to best suit the molecular potential through a simple minimization procedure.

Keywords: vibrational spectra, algebraic method, Morse oscillator, quasi number state basis, basis optimization, anharmonic vibrations.

1 Introduction

In a previous work,¹ an algebraic method for the computation of vibrational spectra of diatomic molecules was introduced. Although this is a 1-dimensional (1D) problem, thus an in principle trivial task, the algebraic method shows substantial advantages over both the real-space grid solution of the Schrödinger equation and harmonic-oscillator-based techniques. These advantages are especially important for extensions to the multidimensional problem of polyatomic vibrations.

The expansion of the molecular potential in powers of the Morse-potential related quantity $v(x) = e^{-\alpha(x-x_0)} - 1$, namely

$$V_d(x) = \sum_{k=2}^{N_{\max}} a_k (v(x))^k, \quad (1)$$

allows an efficient and accurate approximation of a well-behaved molecular potential in the whole energy range, from the minimum region to the dissoci-

ation threshold, generally involving a moderate number $N_{\max} + 1$ parameters a_2, \dots, α and x_0 . Even potentials substantially distorted with respect to the Morse potential can be treated successfully. With the potential expressed in the form of Eq. (1), the complete Hamiltonian

$$\hat{H} \equiv -\frac{\hat{p}_x^2}{2\mu} + V_d(x) \quad (2)$$

(here μ is the reduced mass of the 2-body problem and x is the radial coordinate) can be represented on a quantum-mechanical basis of choice.

The accuracy and efficiency of the direct diagonalization methods rely both on the accuracy of the potential approximation of Eq. (1) and on the properties of the selected basis. The basis had better be complete but also manageable, i.e. related to the algebraic properties of $v(x)$, so that the evaluation of the matrix elements can be done rapidly and without approximations: this will be needed especially in view of extensions to polyatomic molecules.

2 The Basis

Previous research^{1,2,3} showed that the basis

$$\phi_n(y) = \sqrt{\frac{\alpha n!}{\Gamma(2\sigma + n)}} y^\sigma e^{-\frac{y}{2}} L_n^{2\sigma-1}(y), \quad \sigma > 0, \quad n = 0, 1, 2, \dots, \quad (3)$$

with

$$y(x) = (2s + 1) e^{-\alpha(x-x_0)}, \quad (4)$$

can be usefully employed in general diatomic contexts, with the special choice

$$\sigma = s - [s], \quad (5)$$

where $[s]$ indicates the integer part of s , and with s related to the Morse term $a_2(v(x))^2$ in the potential expansion (1), by

$$s = \frac{\sqrt{2\mu a_2}}{\hbar\alpha} - \frac{1}{2}. \quad (6)$$

With the conditions (5,6) the basis (3) was named *quasi number state basis* (QNSB).² In the present work, we only assume α and x_0 in Eqs. (3,4) are the same as in the potential expansion (1), and that $\sigma > 0$ and $s > -\frac{1}{2}$, but release all additional unnecessary conditions on σ and s , for example those expressed by Eqs. (5,6), or the condition defined by Tennyson and Sutcliffe^{4,5} (TS):

$$\sigma = \frac{[2s] + 2}{2}, \quad (7)$$

with s fixed by Eq. (6). Equation (3) thus defines a (s, σ) -parameterized family of bases, *generalized* QNSB (GQNSB), all sharing the following main

features: (i) the basis (3) is complete; (ii) the kinetic and potential operators can be written in terms of generalized ladder operator as specified below, so that (iii) the matrix elements of a vast class of relevant operators is computable easily and exactly by means of simple algebraic relations.¹

Even though all infinite GQNSB's are substantially equivalent, regardless of s and σ , different bases characterized by different values of s and σ show different performances when truncated to a finite number N_s of states and applied to a given quantum mechanical problem specified by $\mu, \alpha, a_2, a_3, \dots, a_{N_{\max}}$. Indeed, the purpose of the present work is to demonstrate that a properly chosen truncated GQNSB can improve the efficiency of the computation substantially, compared to earlier choices.^{1,4}

3 Matrix elements

We follow here the same approach¹ derived from SUSY quantum mechanics.^{2,6} We introduce the generalized Morse ladder operators^{1,2}

$$\begin{aligned}\hat{A}(q) &= q\hat{I} - \frac{\hat{y}}{2} + \frac{i}{\hbar\alpha}\hat{p}_x \\ \hat{A}^\dagger(q) &= q\hat{I} - \frac{\hat{y}}{2} - \frac{i}{\hbar\alpha}\hat{p}_x,\end{aligned}\tag{8}$$

parameterized by the real quantity q .⁷ These operators, with a suitable choice of q , act on the states (3) of the GQNSB as ladder operators:

$$\hat{A}(\sigma + n) \phi_n = C_n \phi_{n-1} \quad (9)$$

$$\hat{A}^\dagger(\sigma + n) \phi_n = C_{n+1} \phi_{n+1},$$

where

$$C_n = \sqrt{n(n + 2\sigma - 1)}. \quad (10)$$

According to Eqs. (8,9), σ links the parameterized basis (3) to the corresponding family of generalized ladder operators. Thus, each and every basis of the form of Eq. (3) can be managed algebraically in this formalism, for any given choice of $\sigma > 0$. In practice, the eigenfunctions (3) depend explicitly on s, α and x_0 , beside σ . We fix x_0 to the position of the minimum of the potential (1), as it would not provide a substantial advantage otherwise. Likewise, we select for α the same value as in the potential expansion, because otherwise all relevant matrix representations would be dense rather than sparse.⁸ With these constraints on x_0 and α , an arbitrary s can be usefully employed in the basis definition: for any s value, the momentum operator p_x and the multiplication operator $e^{-\alpha(\hat{x}-x_0)}$ can be written in terms

of the ladder operators (8):

$$e^{-\alpha(\hat{x}-x_0)} = \frac{2q\hat{I} - [\hat{A}^\dagger(q) + \hat{A}(q)]}{(2s+1)}, \quad (11)$$

$$\hat{p}_x = \frac{\hbar\alpha}{2i} [\hat{A}(q) - \hat{A}^\dagger(q)], \quad (12)$$

where also the \hat{A} operators depend implicitly on the s parameter appearing in the definition (4) of \hat{y} . On the GQNSB (3), the matrix elements of any physical operator expressed as a polynomial of $e^{-\alpha(\hat{x}-x_0)}$ and p_x can be computed algebraically since Eqs. (11,12) express them in terms of the ladder operators of the corresponding specialized basis. We derive here explicitly the algebraic form of the Morse Hamiltonian for general q and s .

Using Eq. (12), the kinetic operator $\hat{K} = \frac{\hat{p}_x^2}{2m}$ becomes

$$\hat{K} = -\frac{\hbar^2\alpha^2}{8m} [\hat{A}^2(q) + \hat{A}^{\dagger 2}(q) - \hat{A}(q)\hat{A}^\dagger(q) - \hat{A}^\dagger(q)\hat{A}(q)]. \quad (13)$$

By applying the commutation relations

$$[\hat{A}(q), \hat{A}^\dagger(q')] = (q+q')I - (\hat{A}(q) + \hat{A}^\dagger(q')), \quad (14)$$

$$[\hat{A}(q), \hat{A}(q')] = [\hat{A}^\dagger(q), \hat{A}^\dagger(q')] = 0,$$

\hat{K} reduces to

$$\hat{K} = -\frac{\hbar^2 \alpha^2}{8m} [\hat{A}^2(q) + \hat{A}^{\dagger 2}(q) - 2q\hat{I} + \hat{A}(q) + \hat{A}^\dagger(q) - 2\hat{A}^\dagger(q)\hat{A}(q)]. \quad (15)$$

Likewise, powers of $e^{-\alpha(\hat{x}-x_0)}$ appearing in the potential-energy operator are obtained starting from Eq. (11). For example,

$$\begin{aligned} e^{-2\alpha(\hat{x}-x_0)} &= \quad (16) \\ &= \frac{1}{(2s+1)^2} \{4q^2\hat{I} - 4q[\hat{A}^\dagger(q) + \hat{A}(q)] + \hat{A}^2(q) + \hat{A}^{\dagger 2}(q) + \hat{A}(q)\hat{A}^\dagger(q) + \hat{A}^\dagger(q)\hat{A}(q)\} \\ &= \frac{1}{(2s+1)^2} \{2(2q^2 + q)\hat{I} - (4q+1)[\hat{A}^\dagger(q) + \hat{A}(q)] + 2\hat{A}^\dagger(q)\hat{A}(q) + \hat{A}^2(q) + \hat{A}^{\dagger 2}(q)\}. \end{aligned}$$

Thus, the Morse-potential term reads

$$\begin{aligned} (v(\hat{x}))^2 &= \frac{1}{(2s+1)^2} \{2(2q^2 + q)\hat{I} - (4q+1)[\hat{A}^\dagger(q) + \hat{A}(q)] + 2\hat{A}^\dagger(q)\hat{A}(q) \\ &\quad + \hat{A}^2(q) + \hat{A}^{\dagger 2}(q)\} - \frac{2}{(2s+1)} \{2q\hat{I} - [\hat{A}^\dagger(q) + \hat{A}(q)]\} \\ &= \frac{1}{(2s+1)^2} \{(4q^2 - 2q - 8sq)\hat{I} + (4s - 4q + 1)[\hat{A}^\dagger(q) + \hat{A}(q)] \\ &\quad + 2\hat{A}^\dagger(q)\hat{A}(q) + \hat{A}^2(q) + \hat{A}^{\dagger 2}(q)\}. \quad (17) \end{aligned}$$

Accordingly, the Morse Hamiltonian $\hat{H}_M = \hat{K} + a_2(v(\hat{x}))^2$ is expressed in

algebraic form as

$$\begin{aligned}
\hat{H}_M &= \left[\frac{2a_2}{(2s+1)^2} + \frac{\hbar^2 \alpha^2}{4m} \right] \hat{A}^\dagger(q) \hat{A}(q) + q \left[\frac{2a_2}{(2s+1)^2} (2q-1-4s) + \frac{\hbar^2 \alpha^2}{4m} \right] \hat{I} \\
&+ \left[\frac{a_2}{(2s+1)^2} (4s-4q+1) - \frac{\hbar^2 \alpha^2}{8m} \right] [\hat{A}^\dagger(q) + \hat{A}(q)] \\
&+ \left[\frac{a_2}{(2s+1)^2} - \frac{\hbar^2 \alpha^2}{8m} \right] [\hat{A}^2(q) + \hat{A}^{\dagger 2}(q)]. \tag{18}
\end{aligned}$$

The representation of Eq. (18) shows that the Morse Hamiltonian is generally 5-band diagonal on a GQNSB of the form (3). We stress that the expression (18) holds for *any* choice of parameters s and q , regardless of them being connected to any specific physical constraint.

If the condition

$$\frac{a_2}{(2s+1)^2} = \frac{\hbar^2 \alpha^2}{8m} \tag{19}$$

(equivalent to Eq. (6)) is satisfied, then the last term, proportional to $[\hat{A}^2(q) + \hat{A}^{\dagger 2}(q)]$ drops from \hat{H}_M . In other words, the choice of the parameter s of Eq. (6) makes the Morse Hamiltonian *tridiagonal* on the corresponding GQNSB basis, irrespective of q . Under this special condition (19), the Morse Hamiltonian simplifies to:

$$\hat{H}_M = \frac{4a_2}{(2s+1)^2} \left\{ [\hat{A}^\dagger(q) + \hat{A}(q)] (s-q) + \hat{A}^\dagger(q) \hat{A}(q) + (q^2 - 2qs) \hat{I} \right\}. \tag{20}$$

The form of Eq. (20), indicates that by further setting

$$q = s, \tag{21}$$

the operator form of the Hamiltonian simplifies even more, and the Morse Hamiltonian factorizes as:

$$\hat{H}_M = 4 \frac{a_2}{(2s+1)^2} [\hat{A}^\dagger(s) \hat{A}(s) - s^2 \hat{I}], \tag{22}$$

which recovers the algebraic form of the Morse Hamiltonian of previous works.^{1,2}

The use of different values of q and s produces a GQNSB, where the algebraic computation of the matrix elements of the Hamiltonian (2) is not significantly more intricate: in particular on a GQNSB, the Morse Hamiltonian is 5-band diagonal, rather than tridiagonal,⁹ and higher powers of $(v(x))^k$ in Eq. (1) generate $(2k+1)$ -band diagonal matrices (like in the QNSB).

For practical potentials, usually substantially distorted from the pure-Morse $(v(x))^2$ term, the actual eigenfunctions can be represented poorly by the $[s]+1$ Morse bound states, or equivalently by their QNSB counterparts: to achieve a good convergency of all eigenfunctions, the QNSB often needs to be complemented by a large number of states, far beyond $[s]+1$. A suitably

chosen GQNSB can thus prove significantly more efficient, especially in a multi-oscillator polyatomic context.

4 GQNSB parametric dependency

The shape of the wavefunctions (3) depends on the four parameters x_0, α, s and σ : different shapes imply different convergence properties when employed to build the matrix representation of the Hamiltonian. A brief analysis of the dependency of the shape of GQNSB states on the various parameters can be useful to gain some insight in their role. Figure 1 shows the profile of three states of the form (3), under conditions (5) and (6). Note that the $n = 0$ state is located substantially at the right of the Morse equilibrium position x_0 , and that further states move in toward x_0 for increasing n . This contrasts with the behavior of a basis of energy eigenstates of a well centered in x_0 . Figure 2 illustrates the behavior of a GQNSB wavefunction, Eq. (3), after variation of the parameters s and σ involved relative to the QNSB values, Eqs. (5, 6). The dependence on the s parameter (Fig. 2a) is weak: by increasing s , the eigenfunction shifts almost rigidly towards the outer region. The σ -dependence (Fig. 2b) is less trivial: for larger σ , the wavefunction deforms and shrinks, concentrating toward the region of the minimum, and decaying more rapidly at large x . The role of the σ parameter is particularly

important: as the n^{th} GQNSB wavefunction (3) has the general form

$$\phi_n(y) \propto e^{-y/2} y^\sigma \text{Pol}[y, n], \quad (23)$$

($\text{Pol}[y, n]$ stands for a polynomial of degree n in the variable y), σ controls the *decay rate of the wavefunctions* for $y \rightarrow 0$, i.e. at the dissociation region. In particular, by choosing small σ , the basis wavefunctions spread away from the well region thus improving the convergency of high-energy states, possibly at the expense of quality of the low-energy states in the well. Equation (23) and Fig. 2 show that the general shape and in particular the amount of localization of the GQNSB wavefunctions can be tuned freely by choosing suitable s and σ parameters: this allows improving the variational efficiency of a truncated GQNSB for a specific quantum-mechanical problem.

5 Optimization of the basis parameters

Assume that the exact N_b bound state eigenvalues E_i^{ex} of the Hamiltonian are known; we can measure the RMS discrepancy of the discrete spectrum due to basis-incompleteness by

$$\tilde{\Delta}^2 = \frac{1}{N_b} \sum_{n=0}^{N_b-1} (E_n - E_n^{\text{ex}})^2, \quad (24)$$

in terms of the numerical eigenvalues E_i , obtained by diagonalizing the matrix of \hat{H} , Eq. (2), on a finite GQNSB composed by the first N_s ($> N_b$) states and parameterized by s and σ . For fixed N_s we can search for the optimal s_{\min} and σ_{\min} that make $\tilde{\Delta}$ minimum.

In fact, the *a priori* knowledge of the exact eigenvalues E_i^{ex} is not necessary: due to the variational nature of basis truncation, a “better” basis makes all eigenvalues E_i lower. Accordingly, the optimal s_{\min} and σ_{\min} parameters can be defined as those producing the lowest eigenvalue spectrum for the assigned basis size N_s , i.e. those minimizing

$$\Delta = \frac{1}{N_b} \sum_{n=0}^{N_b-1} E_n. \quad (25)$$

This approach only requires that the number N_b of bound eigenstates is known. Of course, the number N_b of bound states can be determined once and for all, for example by means of a calculation on a very extended QNSB. The minimization of $\tilde{\Delta}$ and of Δ leads generally to slightly different results, but the following qualitative discussion applies equally well to both schemes. Unless specified, for the determination of s_{\min} and σ_{\min} , we minimize Δ as defined in Eq. (25), and compare Δ to its fully-converged value Δ_0 computed on a largely complete basis.

In a typical application of the GQNSB, one starts from a molecular po-

tential energy expressed in terms of an expansion of the form of Eq. (1). Before considering realistic dimers (H_2 and Ar_2), we illustrate the properties of the optimized GQNSB for a simple toy potential defined by

$$N_{\max} = 4, a_2 = a_4 = 625, a_3 = 0, \alpha = 4, \text{ and } x_0 = 1, \quad (26)$$

which we solve combined with a kinetic term specified by $\hbar = 1$, $\mu = 1$. We minimize Δ with respect to s and σ , for two fixed numbers of basis states $N_s = 30$ and 16. Figure 3(a) shows the values of the individual eigenvalue discrepancy $(E_n - E_n^{\text{ex}})/a_2$ for the potential (26), for the QNSB, for an optimized GQNSB (OGQNSB), and for s and σ chosen according to the prescription of TS.^{4,5} The optimized parameters of the $N_s = 30$ OGQNSB are $s_{\min} = 20.01$ and $\sigma_{\min} = 0.435$, to be compared with the QNSB ones $s = 8.338$ and $\sigma = 0.338$, and those chosen according to the prescription of TS^{4,5} $s = 8.338$ and $\sigma = 9$. For this potential $\Delta_0 = -444.90$, and the corresponding $\Delta - \Delta_0$ are $3 \cdot 10^{-6}$ for the OGQNSB (Δ equaling Δ_0 to 5 decimal digits), 0.061 for the QNSB, and 457 for the TS choice. Both QNSB and the OGQNSB retrieve all the bound states, but the OGQNSB produces much better converged eigenenergies, especially near dissociation. The TS basis instead yields only 9 of the 14 bound states, only few of which are converged within $10^{-2} a_2$, which explains the large discrepancy $\Delta - \Delta_0$.

Figure 3(b) shows the same individual discrepancies obtained with a basis of $N_s = 16$ states instead of 30. The s and σ values of the QNSB and the TS basis are of course unchanged, while for the OGQNSB they change to $s_{\min} = 14.47$ and $\sigma_{\min} = 0.314$. The discrepancies $\Delta - \Delta_0$ deteriorate to 0.106, 87.35, and 4045.9 for OGQNSB, QNSB and TS respectively. Clearly the OGQNSB maintains a fair accuracy throughout the spectrum, by allowing for slightly less accurate lowest bound states, at the benefit of those near dissociation. In contrast, the $N_s = 16$ QNSB fails in obtaining the two bound states closest to dissociation, and the TS basis only produces 6 bound states. Thus, basis parameters optimization allows a substantial improvement of the accuracy of the results, with the same computational cost. In other words, the convergence speed of the computation can be improved drastically by means of a suitable choice of s and σ , for example Fig. 3 demonstrates an equal accuracy of the OGQNSB of 16 states and the QNSB of 30 states.

Figure 4 illustrates a typical s dependence of the total discrepancy $\Delta - \Delta_0$: for σ equal to its optimal value σ_{\min} (solid curve), as s approaches the optimal s_{\min} value from below, Δ decreases relatively slowly, while for s increasing beyond s_{\min} , Δ grows very steeply. The σ dependence of Δ has a sharp and roughly symmetrical deep minimum around σ_{\min} .

The reason for the observed s and σ dependencies of Δ is related to the GQNSB wavefunction profiles of Figs. 1 and 2, and Eq. (23). When s

increases, the GQNSB wavefunctions shift almost rigidly toward the dissociation region of the potential. As the GQNSB wavefunctions decay much more rapidly for small x than for large x , approaching s_{\min} from below the accuracy of the representation of the bound states localized in the well region improves slowly, but soon after the optimal s is found, all wavefunctions move their localization region to the right of the equilibrium position, and cease to account well for the eigenstates behavior at the left of x_0 . On the other hand, σ affects mainly the vanishing rate for large x , which affects the bound states representation quite severely, but in a rather symmetric way. Convergency can be quite substantially improved by tuning the wavefunctions localization, and this can be achieved by choosing the most appropriate s and σ , thus precisely the OGQNSB.

6 Examples of Applications

6.1 Ar₂

We compare the OGQNSB and the QNSB for the calculation of the vibrational spectrum of the Argon dimer, for which a reliable *ab-initio* molecular potential is provided¹⁰ in terms of a set of 47 points in the range $x = 0.25$ to 20 Å. Patkowski *et al.*¹⁰ propose an analytic expression fitting the *ab-initio* points rather accurately. We fit the *ab-initio* data instead to the expansion

of Eq. (1), up to degree $N_{\max} = 8$. The resulting best-fit coefficients are reported in Table 1. Since the repulsive small- x region does not affect the bound states significantly anyway, we privilege the convergence inside the binding well region, with a weighted fit.¹¹ Despite its simplicity, generality, and the relatively small number of parameters involved ($N_{\max} + 1 = 9$), the resulting expansion is quite accurate, throughout the whole energy range covered by the 47 *ab-initio* points. In particular, in the well region the agreement is quite good, with a RMS discrepancy δ_{RMS} of less than half wavenumber, see Table 1. Moreover, the resulting model potential does not suffer from the unphysical small- x divergence to $-\infty$ of the fitted function,¹⁰ and rather tracks the repulsive region within few electronvolts. The well depth (classical dissociation energy) is $D_e = \sum_{i=2}^{N_{\max}} (-)^i a_i = 99.23 \text{ cm}^{-1}$.

We apply the algebraic method and solve the resulting quantum-mechanical problem (2) for the bound-state eigenvalues, using QNSB and GQNSB of different size N_s . Table 2 compares the results obtained by finite-differences solution of the Schrödinger equation for the analytic potential by Patkowski *et al.*,¹⁰ and by numerical diagonalization of the algebraic Hamiltonian (2) with the parameters from Table 1 on a large $N_s = 100$ OGQNSB ($s = 80.18$, $\sigma = 0.213$). This large OGQNSB was chosen to ensure that the results are fully converged, and is taken as reference. The excitation energies obtained using our expansion compare favourably to those obtained by using

Patkowski *et al.* analytic expression,¹⁰ and to the experimental $J = 0$ data,¹² demonstrating equally good or better agreement.

Table 3 illustrates the convergency properties of the unoptimized QNSB by reporting the eigenvalues obtained by diagonalizing the expanded Hamiltonian (2) on $N_s = 100$, 20 and 15 states respectively. The energy differences with respect to the $N_s = 100$ OGQNSB reference are shown, in parentheses, when exceeding 10^{-3} cm^{-1} . Fairly well converged results are obtained even for the small $N_s = 15$ QNSB. Notice however that the bound state closest to dissociation is unbound for $N_s = 15$ and 20, since it is so extended that a rather large QNSB ($N_s \geq 42$) is needed to obtain it at negative energy. Even the very large $N_s = 100$ QNSB does not provide a well-converged result for that specific level.

By diagonalizing the expanded Hamiltonian (2) on $N_s = 20$ and $N_s = 15$ OGQNSB, we obtain the complete spectrum, and with an accuracy $\Delta - \Delta_0$ of $6 \cdot 10^{-5}$ and 0.013 cm^{-1} respectively. The accuracy of all bound levels but the last one is basically the same as for the corresponding QNSB, but the complete discrete spectrum is obtained, including the highest level. The accuracy of the $N_s = 15$ OGQNSB is therefore better than that of $N_s = 100$ QNSB, for Ar_2 . Reducing the basis size below $N_s = 15$, the highest state is missing, but the GQNSB can still be tuned to obtain a fair accuracy of all other states ($\Delta - \Delta_0 < 0.5 \text{ cm}^{-1}$ for $N_s \geq 11$).

6.2 H₂

In a previous work¹ we applied the QNSB formalism to the *ab-initio* adiabatic potential^{13,14} for the H₂ molecule. We found that an expansion (1) up to $N_{\max} = 12$ fits all 169 available *ab-initio* points with a deviation $\delta_{RMS} = 5.5 \text{ cm}^{-1}$. This expansion, whose parameters are reported in Table IV of Ref.¹, produces all the 15 vibrational bound states of this molecule. The QNSB parameters for this potential are $s = 25.56$ and $\sigma = 0.564$. The QNSB produces a cm^{-1} converged spectrum using $N_s \geq 28$ basis states.

By minimizing $\tilde{\Delta}$, Eq. (24), we generate an OGQNSB of smaller N_s . For the calculation of $\tilde{\Delta}$ we use the fully converged $N_s = 200$ QNSB results as reference, reported in the second column of Table 4. A $N_s = 25$ OGQNSB with $s = 26.36$ and $\sigma = 2.115$ ($\tilde{\Delta} = 0.173 \text{ cm}^{-1}$) produces eigenvalues with the same cm^{-1} figures, i.e. the same accuracy of the $N_s = 28$ QNSB: since they are identical to the second column of Table 4, they are not shown. For less strict accuracy requirements, one could reduce the basis size: the last two columns of Table 4 compare the eigenvalues obtained with $N_s = 21$ QNSB and OGQNSB. The H₂ potential expansion illustrates the robustness of the GQNSB in state-poor situations: here, for the $N_s = 21$ QNSB eigenvalues the differences with respect to the fully converged values reach hundreds of wavenumbers, with a RMS discrepancy $\tilde{\Delta} = 323 \text{ cm}^{-1}$, while the discrep-

ancy of the eigenvalues obtained by diagonalizing on the $N_s = 21$ OGQNSB amounts to $\tilde{\Delta} = 3.7 \text{ cm}^{-1}$ only.

7 Conclusions

The substantial improvement of the variational accuracy of the bound-state spectra computed on a OGQNSB w.r.t. the unoptimized QNSB permits in practice to make calculations of a given accuracy on a significantly smaller basis size. While this improvement is practically irrelevant to the solution of the 1-dimensional vibrational problem of diatomics, it is of great importance for the application of this method to the calculation of the spectra based on the *ab-initio* multi-dimensional potential surfaces of polyatomic molecules, as is currently pursued in quantum chemical research.^{15,16,17,18,19,20} We are currently testing the generalization of the expansion (1) to the polyatomic case.²¹

Acknowledgement

We thank Konrad Patkowski for kindly providing us with the complete *ab-initio* Ar₂ PES data including those not available in his paper.¹⁰

References and Notes

- (1) Bordoni, A.; Manini, N. *Int. J. Quant. Chem.* **2007**, *107*, 782.
- (2) Molnár, B.; Földi, P.; Benedict, M. G.; Bartha, F. *Europhys. Lett.* **2003**, *61*, 445.
- (3) Lemus, R.; Arias, J. M.; Gómez-Camacho, J. *J. Phys. A : Math. Gen.* **2004**, *37*, 1805.
- (4) Tennyson, J.; Sutcliffe, B. T. *J. Chem. Phys.* **1982**, *77*, 4061.
- (5) Tennyson, J.; Kostin, M. A.; Barletta, P.; Harris, G. J.; Polyansky, O. L.; Ramanlal, J.; Zobov, N. F. *Comp. Phys. Comm.* **2004**, *163*, 85.
- (6) Cooper, F.; Khare, A.; Sukhatme, U. P. *Phys. Rep.* **1995**, *251*, 268.
- (7) One could even consider different q for the A and A^\dagger operators, but such more general choice does not seem particularly interesting for molecular applications: we take a single q .
- (8) The use of an α basis-parameter different from the potential one affects the matrix elements substantially. This is seen through the recursive relations for the matrix elements,² specialized to the present case (sub-

script B and P stand for basis and potential respectively)

$$\begin{aligned} \langle \phi_m | e^{-\frac{\alpha_P}{\alpha_B} \alpha_B (\hat{x} - x_0)} | \phi_{n+1} \rangle &= [C_m \langle \phi_{m-1} | e^{-\frac{\alpha_P}{\alpha_B} \alpha_B (\hat{x} - x_0)} | \phi_n \rangle + \\ &\quad (n - m - \frac{\alpha_P}{\alpha_B}) \langle \phi_m | e^{-\frac{\alpha_P}{\alpha_B} \alpha_B (\hat{x} - x_0)} | \phi_n \rangle] / C_{n+1}, \\ \langle \phi_0 | e^{-\frac{\alpha_P}{\alpha_B} \alpha_B (\hat{x} - x_0)} | \phi_0 \rangle &= \frac{\Gamma(2\sigma + \frac{\alpha_P}{\alpha_B})}{(2s + 1)^{\frac{\alpha_P}{\alpha_B}} \Gamma(2\sigma)}, \end{aligned}$$

where the C_n are the coefficient of Eq. (10). This recursion implies that if $\alpha_P \neq k\alpha_B$, for integer k , all matrix elements of integer powers of $e^{-\alpha_P(\hat{x}-x_0)}$ are non-vanishing. Moreover, these recursive relations are more intricate than the algebraic rules holding when α_P/α_B is an integer.

(9) In addition, Eqs. (5) and (6) grant an isomorphism of the Morse-problem bound-states subspace with the subspace generated by the first $[s] + 1$ states of the QNSB;² this isomorphism does not hold for general s and σ .

(10) Patkowski, K.; Murdachaew, G.; Fou, C.-M.; Szalewicz, K. *Mol. Phys.* **2005**, *103*, 2031.

(11) We weight all data points below dissociation proportionally to $1/(100 \text{ cm}^{-1})^2 (\simeq 1/(D_e)^2)$, and those above dissociation proportionally

to $1/(100V_j^2)$, where V_j is the *ab-initio* adiabatic energy of the j -th data point.

- (12) Herman, P. R.; LaRoque, P. E.; Stoicheff, B. P. *J. Chem. Phys.* **1988**, *89*, 4535.
- (13) Schwartz, C.; Le Roy, R. J. *J. Mol. Spectrosc.* **1987**, *121*, 420.
- (14) K olos, W.; Wolniewicz, L. *J. Chem. Phys.* **1968**, *49*, 404.
- (15) Wyatt, R. *J. Chem. Phys.* **1998**, *109*, 10732.
- (16) Pochert, J.; Quack, M.; Stohner, J.; Willeke, M. *J. Chem. Phys.* **2000**, *113*, 2719.
- (17) Callegari, A.; Pearman, R.; Choi, S.; Engels, P.; Srivastava, H.; Gruebele, M.; Lehmann, K. K.; Scoles, G. *Mol. Phys.* **2003**, *101*, 551.
- (18) Handy, N. C.; Carter, S. *Mol. Phys.* **2004**, *102*, 2201.
- (19) Zobov, N. F.; Ovsyannikov, R. I.; Shirin, S. V.; Polyansky, O. L. *Opt. Spectrosc.* **2007**, *102*, 348.
- (20) Makarewicz, J.; Skalozub, A. *J. Phys. Chem. A* **2007**, ASAP Article.
- (21) Bordoni, A., *Calculation of Molecular Vibrational Spectra through a Complete Morse Expansion*, *PhD Thesis* **2006**, Univ. Milan, <http://www.mi.infm.it/manini/theses/BordoniPhD.pdf>, Chap. 6.

TABLE 1: Fit quality and parameters for model potential (1), $N_{\max} = 8$, to the Ar₂ potential.

δ_{RMS} [Ha]	0.26
δ_{RMS} well [cm ⁻¹]	0.48
α	$0.516787 a_0^{-1}$
a_2	1359.70868 μ Ha
a_3	1136.96625 μ Ha
a_4	181.96578 μ Ha
a_5	43.51541 μ Ha
a_6	3.77230 μ Ha
a_7	-0.13914 μ Ha
a_8	0.00202 μ Ha
x_0	7.116 a_0

TABLE 2: Energy differences (in cm^{-1}), between consecutive $J = 0$ vibrational levels of Ar_2 .

$i - i'$	numerical ^a	OGQNSB $N_s = 100$	experiment ^b
1-0	25.76	25.64	25.69
2-1	20.49	20.43	20.58
3-2	15.44	15.46	15.58
4-3	10.79	10.90	10.91
5-4	6.75	6.92	6.84
6-5	3.56	3.71	–
7-6	1.36	1.31	–

^aNumerical diagonalization of the Patkowski *et al.*'s potential.¹⁰

^bUltraviolet laser spectroscopy data by Herman et al.¹²

TABLE 3: Bound-state eigenvalues of the Ar_2 dimer, computed with different methods, all based on the *ab-initio* values¹⁰ [in cm^{-1}].

state	OGQNSB $N_s = 100$	QNSB $N_s = 100$	QNSB $N_s = 20$	QNSB $N_s = 15$
0	-84.41	-84.41 (-)	-84.41 (-)	-84.40 (0.005)
1	-58.77	-58.77 (-)	-58.77 (-)	-58.75 (0.01)
2	-38.34	-38.34 (-)	-38.34 (-)	-38.31 (0.02)
3	-22.88	-22.88 (-)	-22.88 (-)	-22.84 (0.04)
4	-11.98	-11.98 (-)	-11.98 (-)	-11.93 (0.05)
5	-5.06	-5.06 (-)	-5.06 (-)	-5.02 (0.04)
6	-1.35	-1.35 (-)	-1.35 (-)	-1.32 (0.02)
7	-0.036	-0.015 (0.02)	0.022 (0.06)	0.051 (0.09)

TABLE 4: H₂ bound-state energies in reduced-size algebraic bases; in parentheses, the differences w.r.t. the reference [in cm⁻¹].

state	QNSB ^a $N_s = 200$	QNSB ^b $N_s = 21$	OGQNSB ^c $N_s = 21$
0	-36113	-36113 (-)	-36113 (-)
1	-31948	-31948 (-)	-31948 (-)
2	-28020	-28019 (1)	-28020 (-)
3	-24324	-24322 (2)	-24324 (-)
4	-20856	-20845 (11)	-20856 (-)
5	-17614	-17573 (41)	-17614 (-)
6	-14599	-14486 (113)	-14598 (1)
7	-11815	-11588 (227)	-11814 (2)
8	-9271	-8907 (365)	-9269 (3)
9	-6979	-6486 (493)	-6975 (4)
10	-4955	-4376 (579)	-4951 (4)
11	-3222	-2626 (596)	-3218 (4)
12	-1810	-1281 (530)	-1806 (5)
13	-761	-389 (372)	-757 (4)
14	-135	-9 (126)	-125 (10)

^aReference fully converged calculation.

^bEigenvalues obtained with a $N_s = 21$ QNSB. The maximum difference of 596 cm⁻¹ corresponds to 1.6% of the well depth.

^cEigenvalues obtained with a $N_s = 21$ OGQNSB ($s = 23.52$, and $\sigma = 3.194$). The maximum difference of 10 cm⁻¹ corresponds to 0.03% of the well depth.

Figure 1. QNSB wavefunctions for $n = 0$, $n = 4$ and $n = 8$, compatible with a Morse problem characterized by $x_0 = 1$, $\alpha = 4/x_0$, $a_2 = 625$, in units where $\mu = 1$, $\hbar = 1$, so that $s = 8.34$, $\sigma = 0.34$.

Figure 2. Variation of the $n = 4$ GQNSB wavefunction for a 50% increase in the parameters s (a), or σ (b), solid line, with respect to the QNSB starting wavefunction (dashed line) corresponding to $s = 8.34$, $\sigma = 0.34$, $x_0 = 1$, $\alpha = 4/x_0$, like in Fig. 1.

Figure 3. Discrepancies $(E_n - E_n^{\text{ex}})/a_2$ of the individual eigenvalues n for the potential $V(x) = a_2[(v(x))^2 + (v(x))^4]$. (a) $N_s = 30$ (OGQNSB with $s_{\text{min}} = 20.01$, $\sigma_{\text{min}} = 0.435$); (b) $N_s = 16$ (OGQNSB with $s = 14.47$, $\sigma = 0.314$), for all bound states. The OGQNSB (diamonds) discrepancies are compared to those based on the QNSB (circles), and to the GQNSB based on the choice of (s, σ) made by Tennyson and Sutcliffe^{4,5} (triangles).

Figure 4. s dependence of Δ Eq. (25), for $V(x)$ defined in Eq. (26), computed with the GQNSB of $N_s = 30$ elements, as a function of s , and for σ fixed to σ_{min} , to $\sigma_{\text{min}} \pm 0.005$, and to $\sigma_{\text{min}} \pm 0.01$.

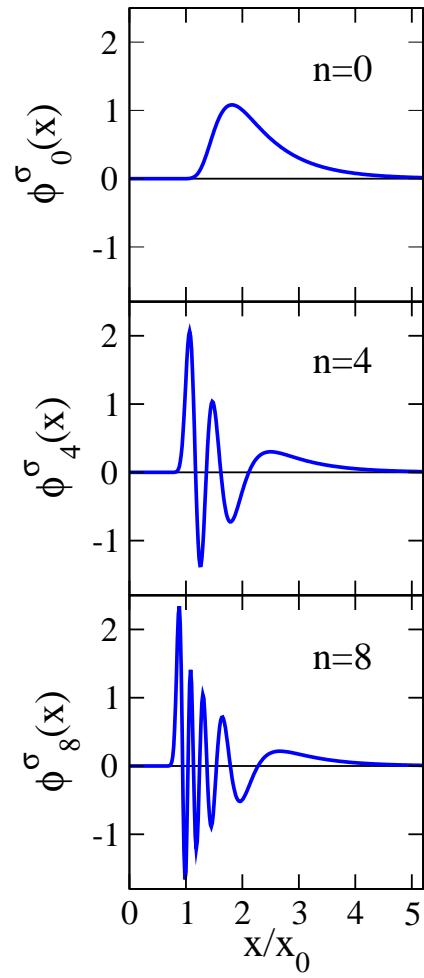


Figure 1.

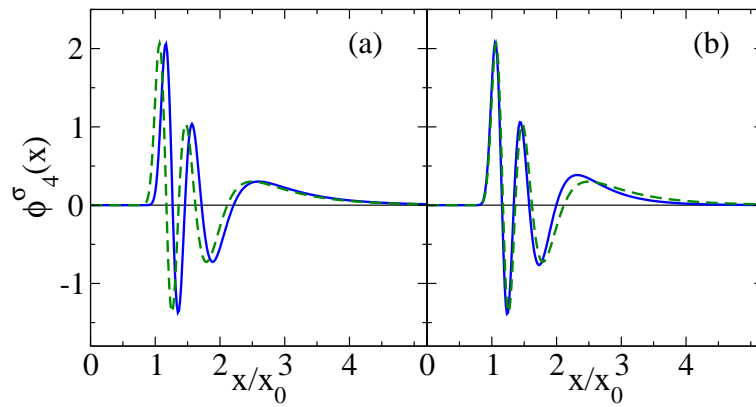


Figure 2.

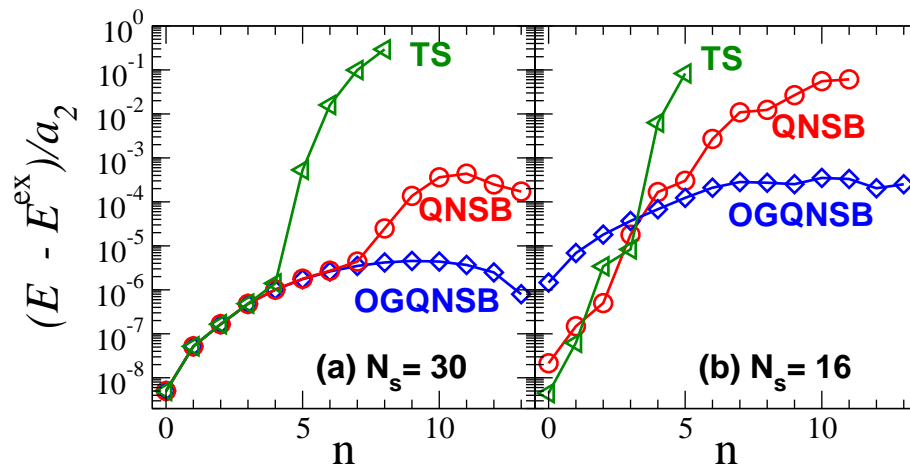


Figure 3.

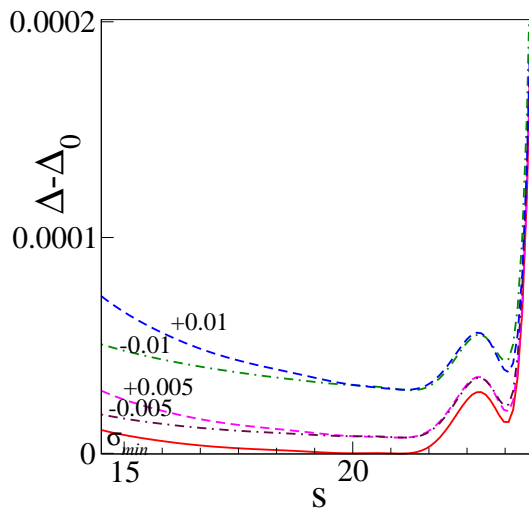


Figure 4.